Electronic Supplementary Material (ESI) for Biomaterials Science.

Supporting Information

Mapping the Time Dependent DNA Fragmentation caused by Doxorubicin Loaded on PEGylated Carbogenic Nano Dot using Fluorescence Lifetime Imaging and Super-resolution microscopy

Chethana Rao[1], Shagun Sharma [1], Richa Garg[1], Farhan Anjum[1,2], Kush Kaushik[1] and Chayan Kanti Nandi[1,2,]*

[1]School of Basic Sciences, Indian Institute of Technology (IIT) Mandi, H.P-175075, India.

[2]BioX Centre, Indian Institute of Technology (IIT) Mandi, H.P-175075, India.

Experimental Section:

Materials. All glassware was washed with aqua regia (3 HCl/1 HNO_3), followed by rinsing several times with double distilled water. Citric acid, urea, EDC and sulpho-NHS, Carboxylic-PEG-amine (Mw-5000), Doxorubicin Hydrochloride, Human plasma (5g) were purchased from Sigma-Aldrich. DMF was purchased from Fisher Scientific. NaOH and KOH were purchased from Merck chemicals. DNA from Salmon Milt was purchased from HiMedia. Double-distilled (18.3 MΩ) deionized water (ELGA PURELAB Ultra) was used throughout the entire process. DMEM medium (Dulbecco's Modified Eagle Medium), HEPES- 4-(2-hydroxyethyl)-1-piperazineethanesulfonic acid, PBS-Phosphate buffer saline, Anti-Anti- Penicillium-Streptomycin, and FBS-Fetal bovine serum was purchased from Gibco, Invitrogen Corporation. HeLa cells were obtained from NCCS Pune India.

Synthesis, Purification, and Characterization of Carbon dot

Synthesis of FND:

The citric acid (1 g) and urea (2 g) were reacted at 180° C for 6 h under a solvothermal condition in 10ml DMF and then cooled to room temperature. The obtained dark brown solution was mixed with 20 ml NaOH (50 mg mL^{-1}), stirred for 1 min, and then centrifuged at 16000 rpm for 10 min (Sorvall LYNX 6000, Thermo Scientific). The precipitate was collected, dissolved in water and centrifuged (16000 rpm, 10 min) twice to wash off residual salts and alkali. The precipitate was dialyzed against Milli-Q water for 8 days using 1 kDa dialysis membrane to remove the free salt and precursors. The water was changed every 24 hours. Finally, the retentate is freeze dried to get the FND.

Synthesis of FND PEG:

For the conjugation of FND with PEG, the carboxyl units on the surface were activated by EDC and NHS. Typically, 12 mg of the freeze-dried FND were made to react with EDC (20 mg) and NHS (20 mg) in 11 ml DMSO. The above solution was left for stirring for 12 h at 1000 rpm at 30˚C. After 12 h, NH_2-PEG (20 mg) in 5 ml DMSO with 1% acetic acid was added and stirred overnight. The solution obtained were made alkaline by the addition of NaOH. The final solution

was centrifuged at 14000 rpm for 30 minutes (twice). It was dialysed against 1KDa membrane to remove any salt or precursor for 24 h. The retentate is freeze dried to get FND PEG.

DOX loading experiments:

In a typical reaction nearly 2mg of FND PEG was dissolved in 1ml of DI water. To the same solution 1.3 mg of DOX was added with constant stirring at an RPM of 100 for 15 hours at room temperature. After 15 hours the solution was centrifuged down at 14000rpm for 30min. The precipitate was washed repeatedly with DI followed by centrifugation. The supernatant was collected each time and stored for calculating drug loading efficiency using UV-Visible spectroscopy. The following formula were used for calculating encapsulation efficiency and percentage drug loading.

Encapsulation efficiency (EE%) = $\frac{Total\ drug\ added - free\ non-trapped\ drug}{Total\ drug\ added}$

Loading capacity (LC%) = $\frac{Amount\ of\ total\ entrapped\ drug}{Total\ nanoparticle\ weight}$

Plasma incubation of the sample:

Approximately 0.5mg of FND and FND PEG sample was incubated with 10% of human plasma purchased from Sigma Aldrich in water for 2 hours at 37^0C. Then the samples were washed 3 times in DI water and centrifuged each time at 14000rpm for 30min. The samples were freeze-dried to find the weight of the sample powders. After plasma incubation the nanoformulations with protein corona were called FND PL and FND PEG PL in order to distinguish them from no corona counterparts.

UV-Vis Absorption and steady state fluorescence spectroscopy:

The UV-Vis absorption spectra were recorded using Shimadzu UV-Vis 2450 spectrophotometer. The spectra were collected using a quartz cuvette having a 10 mm path length and 1 ml volume. All the measurements were repeated at least three times. Steady state fluorescence was measured using a Horiba Fluorolog-3 spectrofluorometer. The fluorescence was measured in 1 ml quartz cuvette.

Transmission Electron Microscopy (TEM): The particle size, dispersity were visualized using a TECNAI G2 200 kV TEM (FEI, Electron Optics) electron microscope with 200 kV input

voltage. TEM grids were prepared by placing 5-10 µL diluted sample solution on a carbon coated copper grid and evaporated the solution at room temperature completely. Precautions were taken to avoid contamination from various sources like dust particles and glassware.

Fourier Transform Infrared Spectroscopy (FTIR):

FTIR spectra of particle were measured using a Perkin-Elmer FTIR spectrophotometer equipped with a horizontal attenuated total reflectance (ATR) accessory containing a zinc selenide crystal and operating at 4 cm^{-1} resolution. The use of the spectral subtraction provided reliable and reproducible results.

X-ray photoelectron spectroscopy (XPS):

X-ray Photo-Electron Spectroscopy (XPS) with Auger Electron Spectroscopy (AES) module PHI 5000 Versa Prob II, FEI Inc. and C60 sputter gun have been used for characterization and scanning the spectra from C1s, N1s, S2p and O1s region. Al Kα X-ray radiation was used as the source for excitation (1486.8 eV, 500 mm). The samples were drop cast on copper strips for measurement.

Fluorescence Correlation Spectroscopy (FCS):

Approx. 50µl sample solutions (~nanomolar concentrations) were drop-casted on a cleaned glass coverslip and placed on an inverted confocal microscope (A1R+, Nikon, Japan) using a 1.4 NA oil-immersion 60X objective for measuring the FCS data. A 561 nm gas laser was used to excite the sample at room temperature (25 °C) using appropriate dichroic and filters in the optical path. The emission beam was directed through a side-port of the microscope delivering it to a Hybrid Photomultiplier Detector Assembly single photon counting module (PicoQuant GmBh. Berlin, Germany). The fluorescence fluctuations were analysed within a point region of interest (ROI) of the sample. The following general autocorrelation function (for n number of diffusion species) was used for fitting and calculating diffusion coefficients.

$$G(t) = \left[1 + T\left[e^{-\left(\frac{t}{\tau_{Trip}}\right)} - 1\right]\right] \sum_{i=0}^{n-1} \frac{\rho(i)}{\left[1 + \frac{t}{\tau_{Diff}[i]}\right]\left[1 + \frac{t}{\tau_{Diff}[i]\kappa^2}\right]^{0.5}}$$

Where τ_{Trip} is the time of triplet blinking and diffusion through the confocal volume. T is triplet contribution and ρ[i] is the contribution of ith species. Our study used the single species model with triplet contribution. The instrument parameter κ was calibrated with a standard fluorophore (RhB) with a known diffusion coefficient. All data were analyzed using the SymPhoTime 64 software (PicoQuant GmBh).

Fluorescence lifetime measurement:

The fluorescence lifetime of bulk solutions were measured using TCSPC instrument from Horba Instruments. The samples were excited using 454 nm pulsed laser and the lifetime was measured at emission maxima of 600 nm for all the samples. To measure the lifetime of DNA-DOX solutions, different concentrations of Salmon Milt DNA is taken in 2 ml DI and same concentration of DOX was added to this. After incubation for 3 h the lifetime was measured.

Cell Culture, live-cell incubation, and fixing:

Cervical cancer line (HeLa) cell lines were grown in Dulbecco's Modified Eagle Medium (DMEM) supplemented with 10% fetal bovine serum (FBS- Gibco, Invitrogen Corporation), 1% Anti-Anti in, 1% HEPES, and 1% NEA (nonessential amino acids- Gibco Invitrogen Corporation) in T-25 flask and incubated in a humidified incubator (at 37°C with 5% CO_2). The density of 1-2 x10^4 cells were seeded in 6-well plates on the coverslips coated with Poly-L-lysin. Each well was filled with 2ml of DMEM growth medium, and the cells were allowed to grow overnight for the proper confluency. The growth and the attachment of the cells to the coverslip were examined by an optical microscope. Once the cells reached actual confluency, they were incubated with samples and plasma incubated samples (25 µg/ml) for an appropriate time (~ 12 h) in the medium. The DOX loaded samples were incubated at a final DOX concentration of 2 µg/ml up to 6 h, 12 h and 24 h. Another set of cells were treated with free DOX of same concentration at these time points. The samples were then washed gently with PBS to remove any nonspecific attachment of the particle on the coverslip to reduce the background and fixed by incubating with 4% paraformaldehyde solution in 1x PBS buffer for 5 min. The DAPI stained cells were prepared by treating cells with triton 0.1 % after fixation for 10 minutes followed by incubated with 15 nM DAPI for 20 minutes. The coverslips were repeatedly washed with PBS to clean them of any free samples. Finally, the coverslips were fixed on a glass slide by using a drop of glycerol and the edges were sealed before imaging.

Cell cytotoxicity:

For cytotoxicity assessment, HeLa cells were seeded in 96 well plates at a density of 5000 cells/well. After overnight incubation, the cells were washed with 1X PBS, and media was replaced with fresh DMEM containing free DOX and DOX loaded particles at a final DOX concentration of 2 µg/ml. After 6, 12 and 24 h of incubation, 40µL of XTT labeling mixture: 5 ml XTT labeling reagent with 0.1 ml electron coupling reagent (Cell proliferation Kit II- XTT Roche) was added to each well and further incubated for 12 h. Tetrazolium salt XTT was cleaved in the presence of an electron-coupling reagent to produce a soluble formazan salts and the absorbance was read at 570 nm with a reference read at 650 nm using Tecan Infinite M200 PRO plate reader.

Coverslip preparation:

The glass slides and coverslips were cleaned by the sonication in ethanol, followed by incubation in HNO_3 and KOH solution for 20 min each and slides were washed by MiliQ water after every step and finally dried by Nitrogen.

Confocal Imaging:

Nikon Eclipse Ti inverted microscope was used for the confocal microscopy and images were acquired using Nikon Nis-Element software. The cell samples were excited by 561nm to achieve imaging and the images were collected with the use of corresponding filters.

Fluorescence Lifetime Imaging Microscopy (FLIM):

Nikon Eclipse Ti inverted Confocal microscope along with Nikon Nis-Element software was used for image acquisition before the FLIM measurement. The FLIM was performed using a time-correlated single photon counting (TCSPC) system PicoHarp 300 and a hybrid PMT System (both from Picoquant Germany) attached to the same confocal microscope. A pulsed diode laser, LDH-P-C-405B, PicoQuant, 405 nm (Pulse FWHM <50ps and Max Repetition rate 40Mhz) was used for the sample excitation and fluorescence signals were collected by choosing a proper dichroic-filter set. Once 60x objective was used for data collection and then 100x oil objective with 1.5x magnification of the microscope were used to collect the data using Nikon microscope. After the data collection, the fluorescence lifetime of entire cell or the ROI firt of

only the nucleus were carried out based on the requirement. The acquired data were fitted using n-exponential reconvolution function for each pixel and finally, the lifetime values were calculated for each ROI. The analysis has been done using Symphotime software provided with the set up.

Super-Resolution Radial Fluctuation Microscopy:

The SRRF is a threshold free algorithm based on the analysis of the image sequence. It considers that the image is convolved with a point spread function (PSF). Each of the PSF created by the single molecules contained a higher degree of local geometrical symmetry than the background. It is better than the single molecule detection because it calculates the local gradient convergence or termed as radiality in the whole frame by dividing each pixel to sub pixels, which preserve the information in the gradient field which would be discarded by any other localization technique. The radiality distribution is independent of the PSF intensity and FWHM of this distribution can be adjusted by gradient convergence radius. The full image created by the radiality distribution can acquire the image noise corresponding to no fluorophore associated radiality peaks, but it can further be de-noised by the time series analysis, the increase in FWHM of the radiality distribution or the radiality map waiting with the fluorophore intensity. In the time series analysis, the higher order temporal cumulants can be calculated and the noise reduction happens because of the uncorrelated noise peaks in the time series and high order correlated peaks at the center of the actual fluorophore. The widefield imaging of was performed using Nikon Eclipse Ti inverted optical microscope in camera mode. A 100X objective (1.49 Oil immersion, Nikon) was used with additional 1.5 magnification to collect fluorescence onto an EMCCD camera (Andor iXon Ultra) and emission was collected in the TRITC filter range. We recorded a time series with 0.05 s acquisition time per image. The movie contained 5000 stacked images, which were analyzed with an open source version of the NanoJ-SRRF on a high performance GPU having 1076 cores. The ring radius chosen for the SRRF analysis was optimized and the best images were obtained at the ring radius 0.5. The chosen radially magnification was 5 times of the original pixel size. Before the SRRF analysis drift correction was done using the correlation method and the final image was displayed as the Temporal Radiality Pairwise Product Mean (TRPPM) method where the final image is the raw second moment of the radiality integrated over the time series and giving a proper noise reduction. The background was calculated from the image area where no molecule was present during the measurement time. The mean value of

this background was subtracted from the original trajectory to obtain a background free signal. Data were processed by the open source NanoJ SRRF plugin of ImageJ. Further the skeletonization and area analysis were done using Image J software plugins.

Analysis using ImageJ:

The original intensity SRRF tif images were cropped to get single-cell images after adjusting the intensity at all time points. Then from each cell image, an ROI (dimesion) was chosen and saved as tif (~ 21 per time point, 11 and 10 respectively from two independent experimental sets). This ROI image was then used to get 3D surface plot, skeletonized, and area outlined images as follows. 3D surface plot is obtained following path, ImageJ-Analyze-3D Surface Plot analysis tool. Skeletonized images are obtained using ImageJ-Plugin-Skeleton-Skeletonize (2D/3D) path. This tool erodes the intensity objects into single pixel values to reveal the interconnected branched structures. The data sheet showing the length measurement is obtained as a Skeletonized image -Image J- Analyze – Skeleton- analyze skeleton. The area outlined images are obtained as ImageJ- Process-Binary-Make Binary; Process-Binary-Outline. The data sheet showing the area measurement is collected as Intensity image-Image J-Analyse-Analyze particles. Finally, the number of clusters with a particular length or area are tabulated manually from the data sheets and plotted in box chart format in origin. The two sample t-test between the two independent set data values at each time point was conducted under the null hypothesis of no significant difference between the two sets using the following t-score equation.

$$\text{t-score} = \frac{\mu_1 - \mu_2}{\sqrt{\frac{(n_1-1){SD_1}^2}{n_1} + \frac{(n_2-1){SD_2}^2}{n_2}}},$$

where, $\mu_1 - \ mean\ for\ the\ first\ sample\ set$

$\mu_2 - \ mean\ for\ the\ Second\ sample\ set$

$n_1 - \ first\ sample\ set\ size$

$n_2 - \ second\ sample\ set\ size$

$SD_1 - \ standard\ deviation\ in\ first\ sample\ set$

$SD_2 - \ standard\ deviation\ in\ second\ sample\ set$

Thickness is measured by collecting the line profiles at the desired positions on the image and fitting them with the Gaussian function in origin. The FWHM of all such fits were collected to make the thickness histogram.

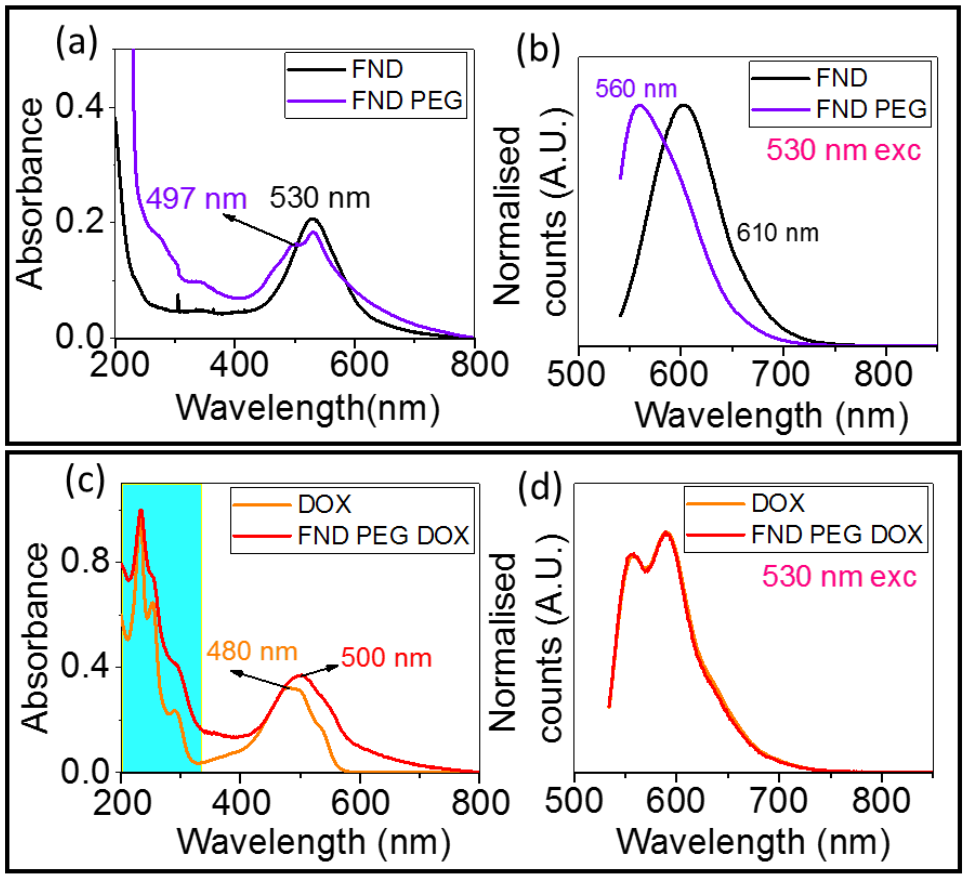

Figure S1: (a) The absorbance and (b) fluorescence emission data comparing FND with FND PEG. (c) The absorbance and (d) fluorescence emission data comparing the DOX with FND PEG DOX.

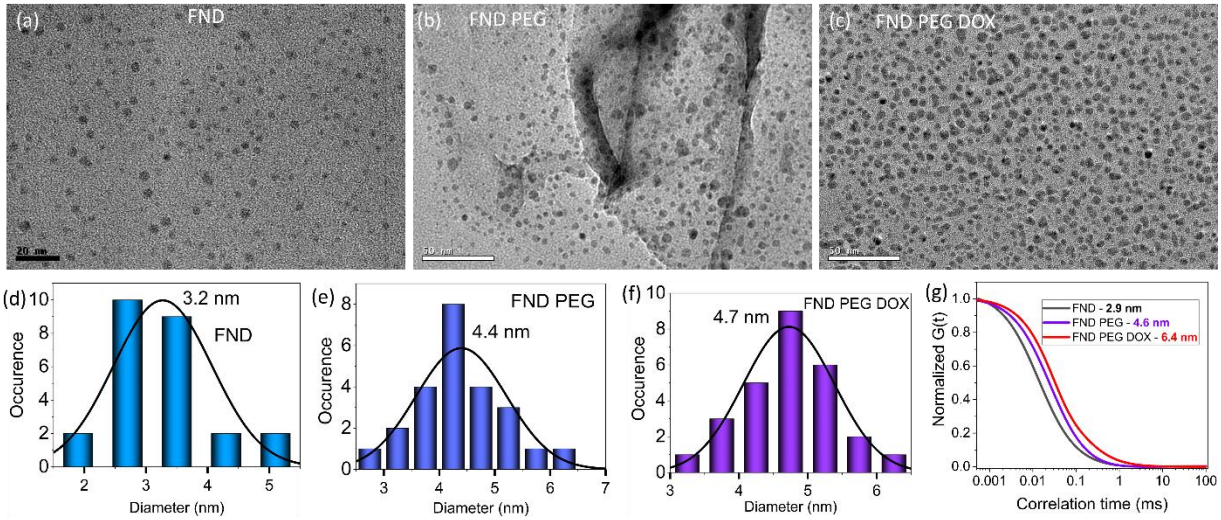

Figure S2: The TEM images for (a) FNDs, (b) FND PEG, (c) FND PEG DOX, showing good morphology even after DOX loading for the particles (Scale bar 20 nm, 50 nm, 50 nm respectively). The size histograms from TEM images for (d) FND (~ 3.2 nm), (e) FND PEG (~ 4.4 nm), (f) FND PEG DOX (~ 4.7 nm). (g) The FCS fitted curves for FND (~ 2.9 nm), FND PEG (~ 4.6 nm), and FND PEG DOX (~ 6.4 nm), show the hydrodynamic diameter for the particles.

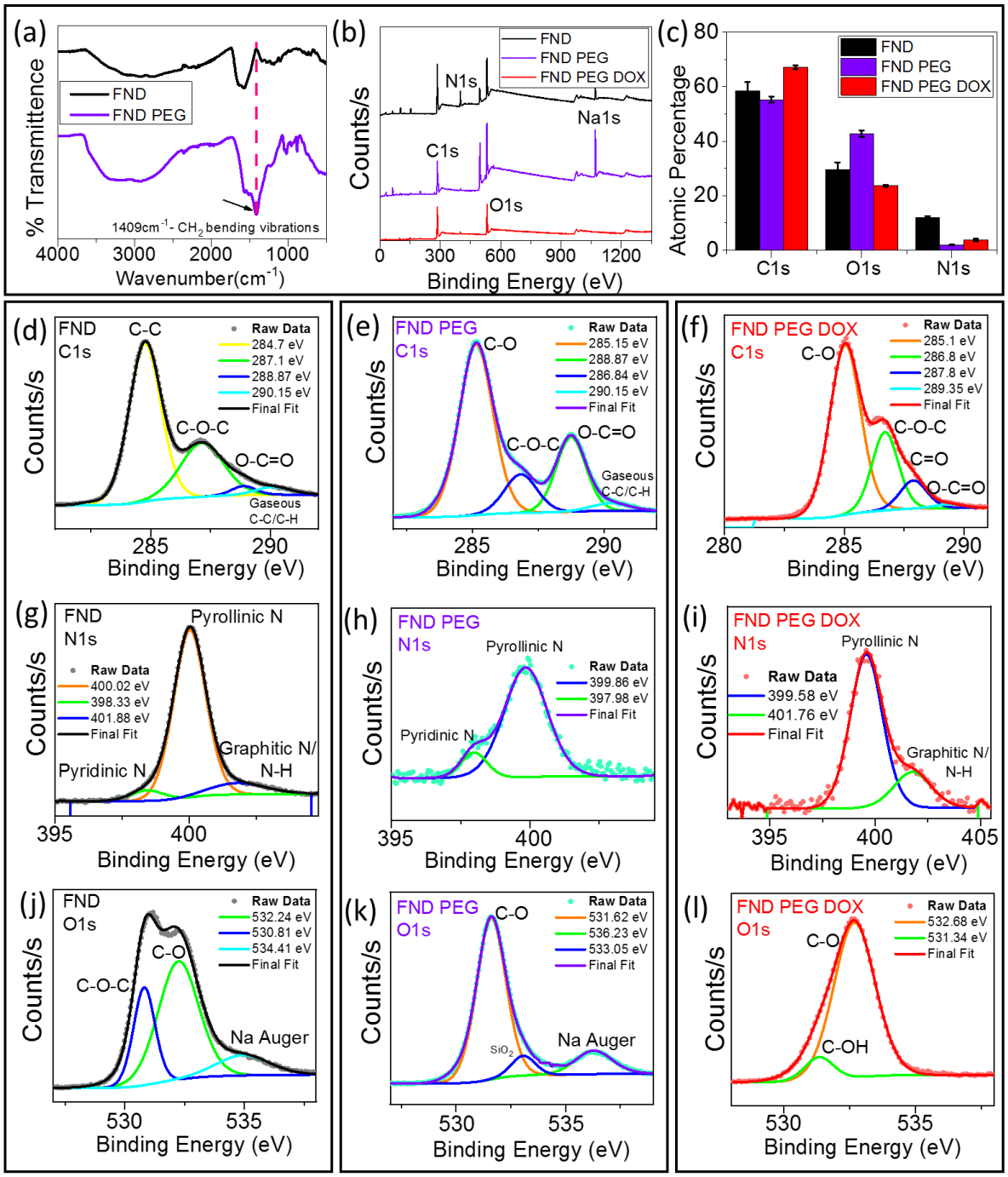

Figure S3: (a) The FTIR spectra and (b) the XPS wide spectra comparing FND, FND PEG and FND PEG DOX. (c) The plot of atomic percentages obtained from XPS for each of them. (d,e,f) The deconvolution of C1s for FND, FND PEG and FND PEG DOX respectively. (g,h,i) The deconvolution of N1s for FND, FND PEG and FND PEG DOX respectively, showing pyridinic, pyrollic Nitrogen. (j,k,l) The deconvolution of O1s for FND, FND PEG and FND PEG DOX respectively, showing dominance of C-O after PEGylation and appearance of C-OH after DOX loading.

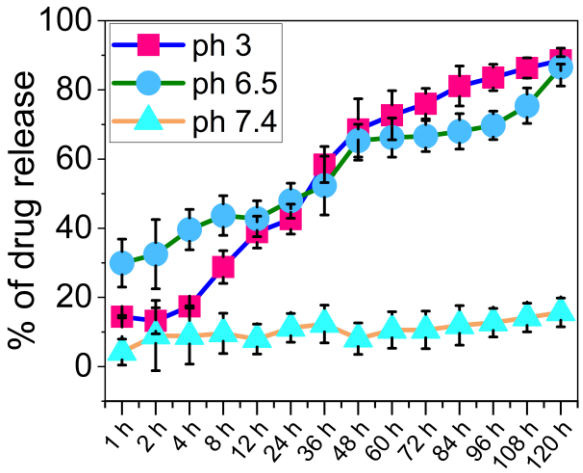

Figure S4: The drug release from FND PEG DOX PL under different buffer pH conditions in bulk solution using dialysis membrane.

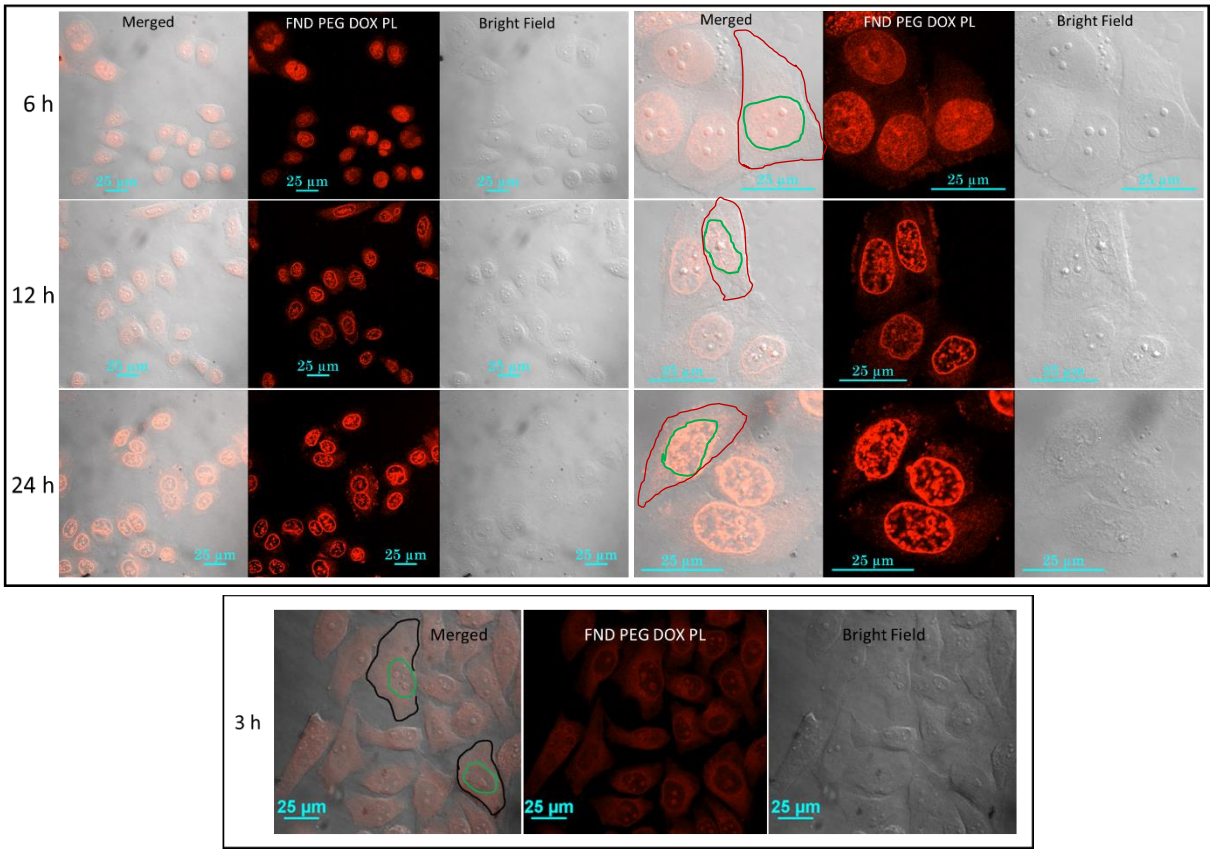

Figure S5: The confocal images showing FND PEG DOX PL treated HeLa cells at the end of 6 h, 12 h and 24 h showing nucleus and cytoplasm staining. The confocal image at 3 h showing nucleolus and cytoplasm staining predominantly. The brightfield and merged images of fluorescence image in Figure 1. The outlines drawn with the help of brightfield images around the nucleus and cytoplasm confirm the staining in different regions.

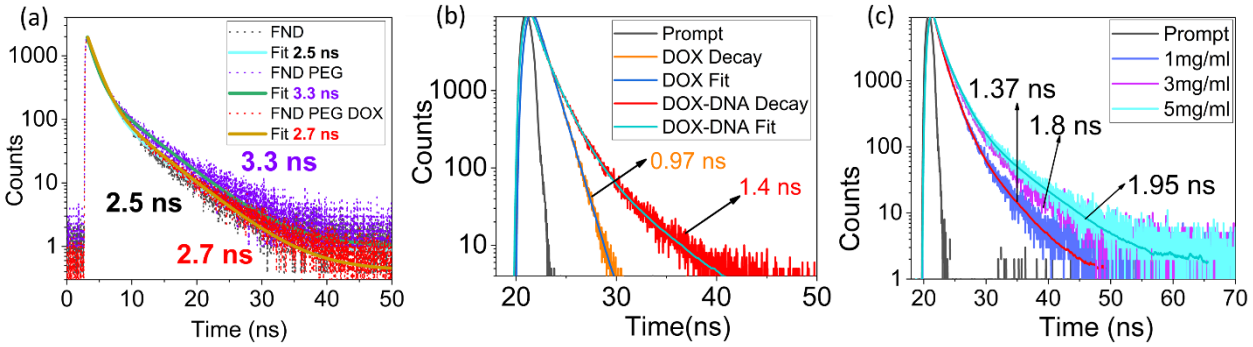

Figure S6: The lifetime data in bulk solution for (a) FND, FND PEG, FND PEG DOX and for (b) free DOX, DOX-DNA, and (c) a fixed concentration of DOX with increasing DNA concentration to elucidate the effects of crowding.

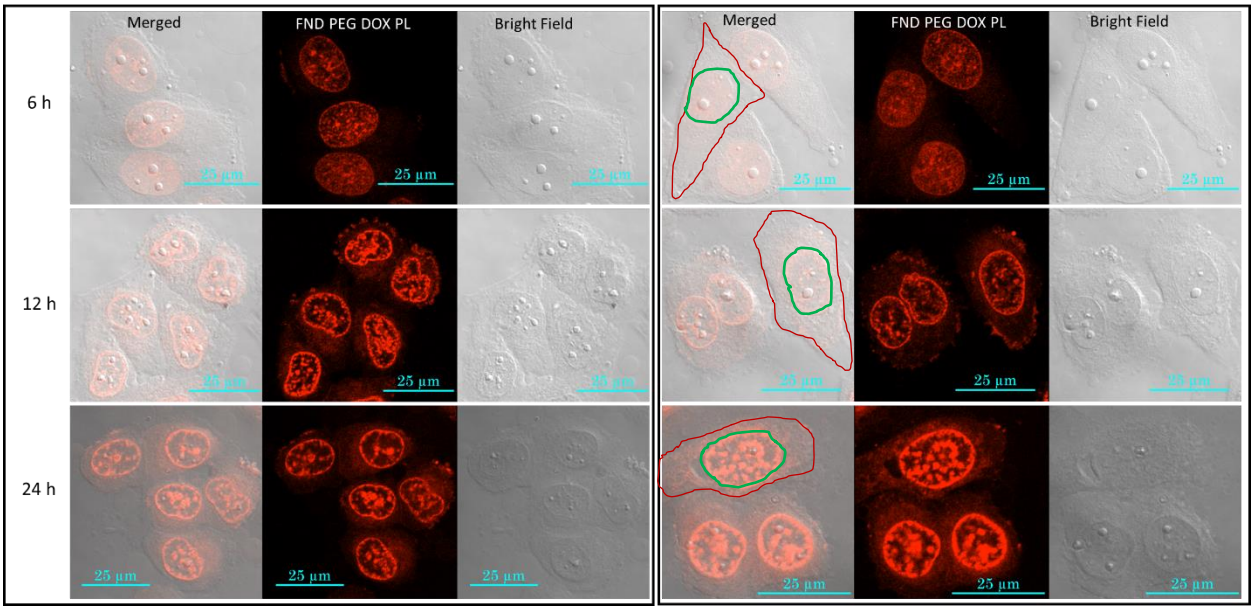

Figure S7: The confocal images corresponding to the FLIM images shown in Figure 2 in the main manuscript of FND PEG DOX PL treated HeLa cells at the end of 6 h, 12 h and 24 h. The outlines drawn with the help of brightfield images around the nucleus and cytoplasm confirm the staining in different regions.

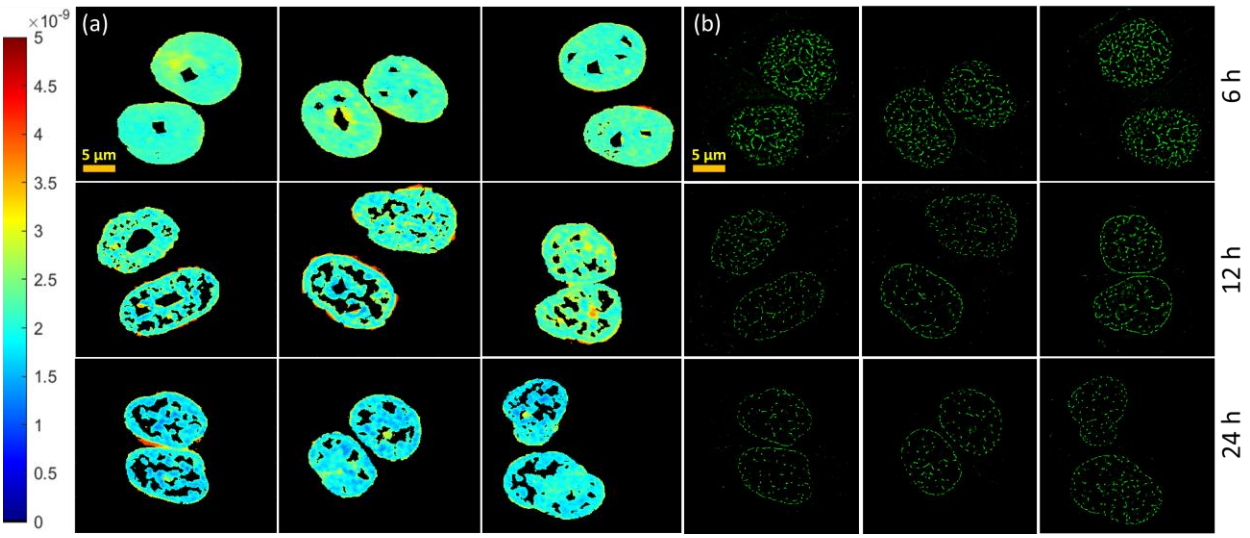

Figure S8: The (a) FLIM and the corresponding (b) SRRF (false color from image j) images of FND PEG DOX PL treated HeLa cells at the end of 6 h, 12 h and 24 h using 100x objective.

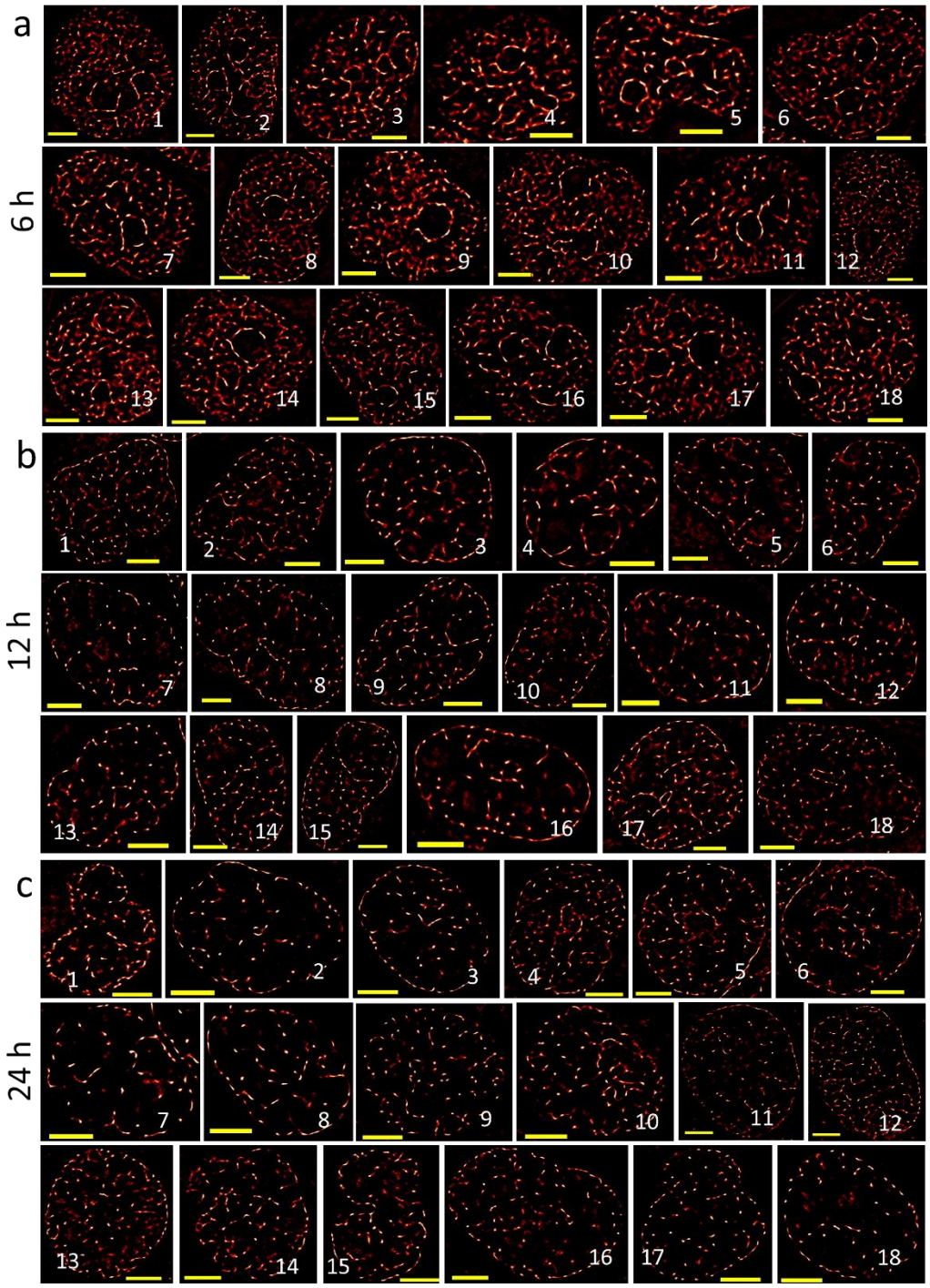

Figure S9: The SRRF images of FND PEG DOX PL treated HeLa cells (n=18 from two independent replicates) at the end of (a) 6 h, (b) 12 h and (c) 24 h using 100x objective (scale bar 3 µm).

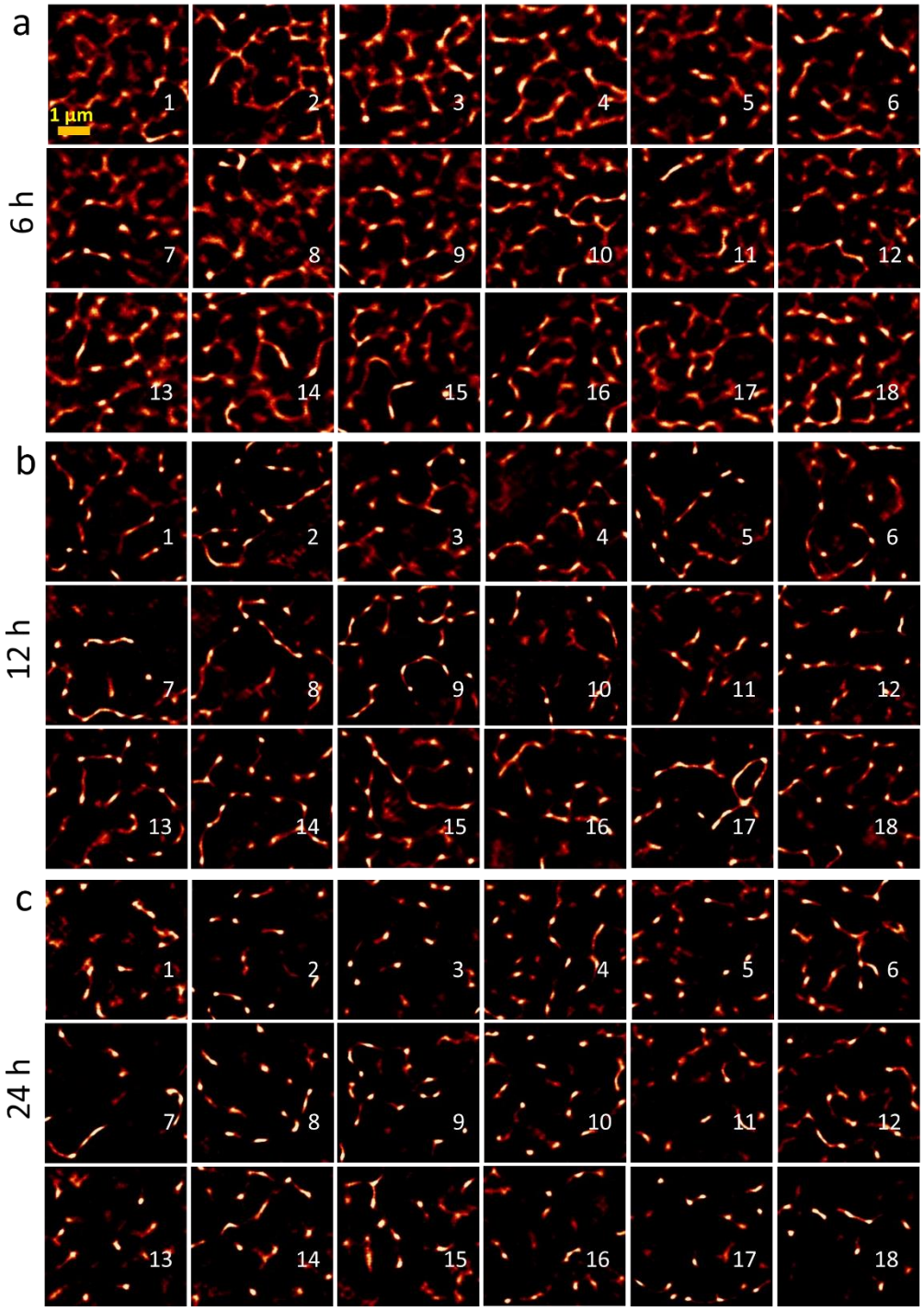

Figure S10: The selected single ROIs from the corresponding full cell SRRF images from Figure S8, of FND PEG DOX PL treated HeLa cells (n=18 from two independent replicates) at the end of (a) 6 h, (b) 12 h and (c) 24 h using 100x objective (scale bar 1 µm, same for all ROIs).

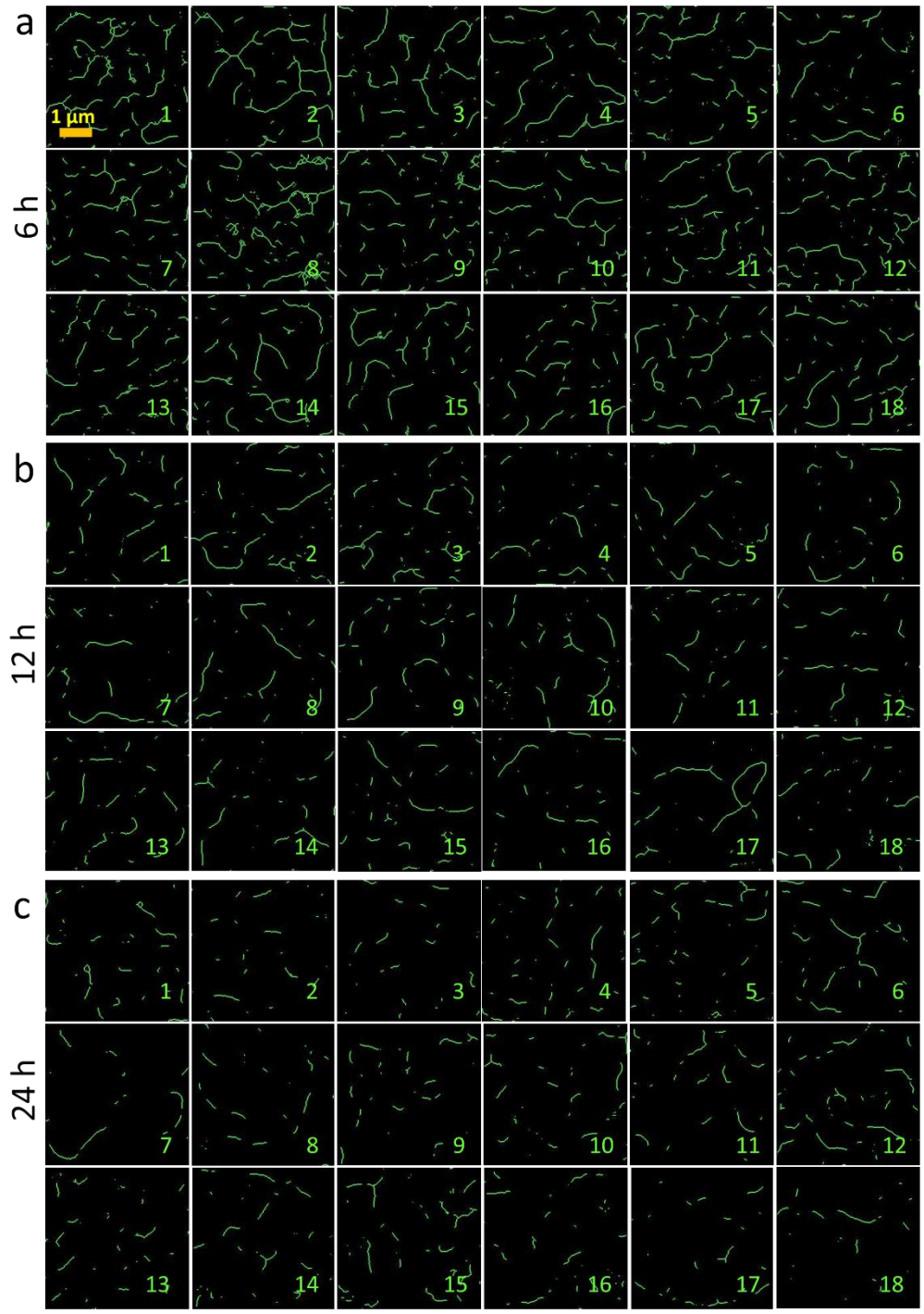

Figure S11: The skeletonized versions of selected single ROIs presented in Figure S9, of FND PEG DOX PL treated HeLa cells (n=18 from two independent replicates) at the end of (a) 6 h, (b) 12 h and (c) 24 h using 100x objective (scale bar 1 µm, same for all ROIs).

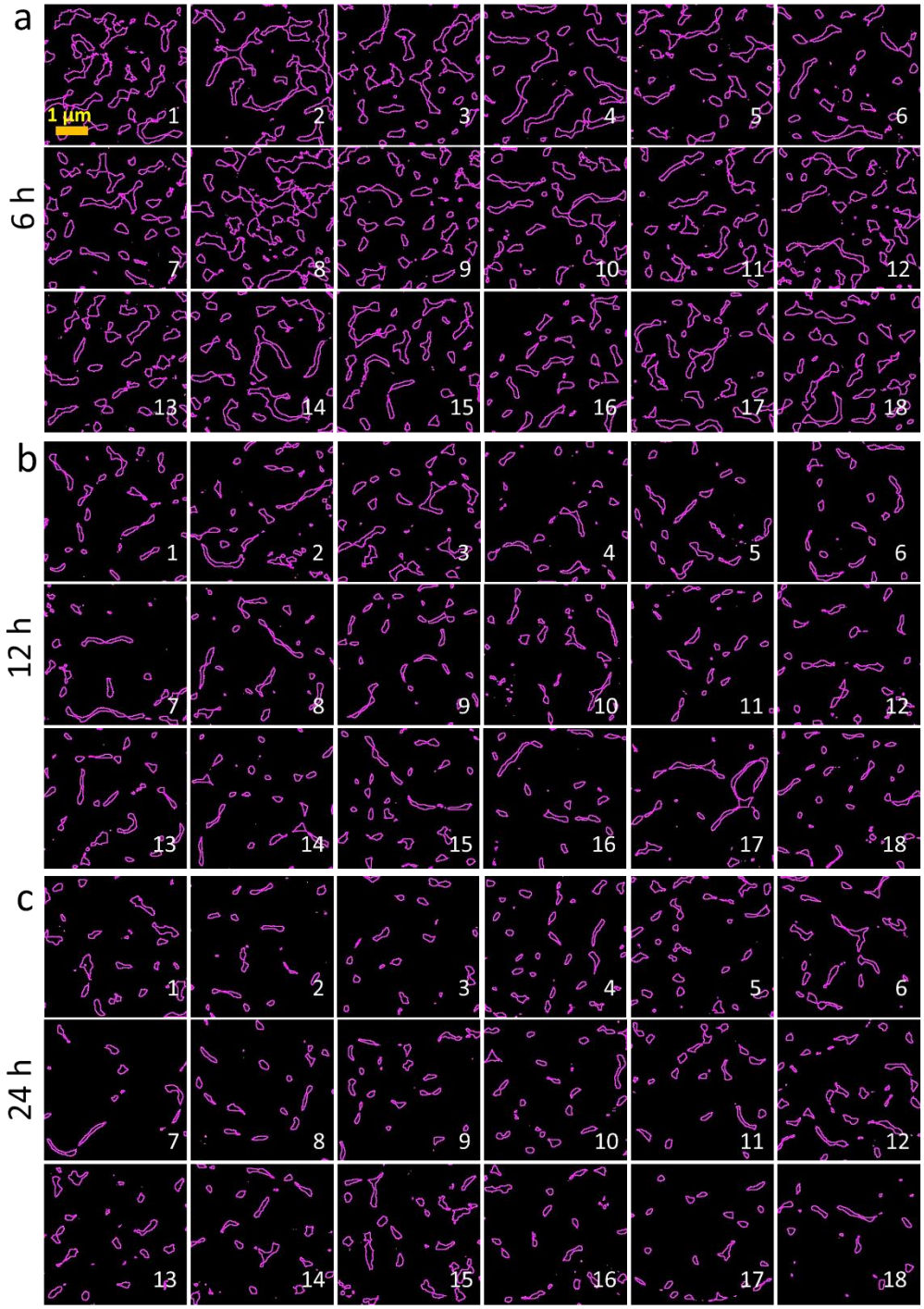

Figure S12: The thresholded, area outlined versions of selected single ROIs presented in Figure S9, of FND PEG DOX PL treated HeLa cells (n=18 from two independent replicates) at the end of (a) 6 h, (b) 12 h and (c) 24 h using 100x objective (scale bar 1 µm, same for all ROIs).

Table S1: The t-score table for the number of clusters with a particular length and area range obtained from two sample t-test. The null hypothesis assumes no difference between the average number of clusters in the given length or area range between two independent experimental sets (total 21 data points). The calculated t-score is then compared with two tailed t-distribution tables at degrees of freedom (11+10-2 = 19) to a value of 2.093 at p = 0.05. All values are found to be less than this value; hence we cannot reject the null hypothesis.

Length		t-score	
		FND PEG DOX PL	DOX
l>500 nm	6 h	-0.21177	-0.39199
	12 h	-1.42359	-0.44028
	24 h	1.196098	-0.37044
500<l<1000	6 h	0.548552	-0.30331
	12 h	-1.12608	-0.31494
	24 h	0.525055	-0.08495
l>1000 nm	6 h	-1.57646	-0.50417
	12 h	0.791817	0.39987
	24 h	1.68741	0.316628
Area		t-score	
		FND PEG DOX PL	DOX
a>100000 nm²	6 h	0.300427	0.178125
	12 h	-1.16671	0.219813
	24 h	-0.10417	-0.12937
100000<a<200000	6 h	-0.85876	0.204973
	12 h	-0.17692	0.003887
	24 h	-0.12106	0.178697
a>200000 nm²	6 h	1.225578	-0.06553
	12 h	-1.60396	0.281105
	24 h	0.067259	-0.42092

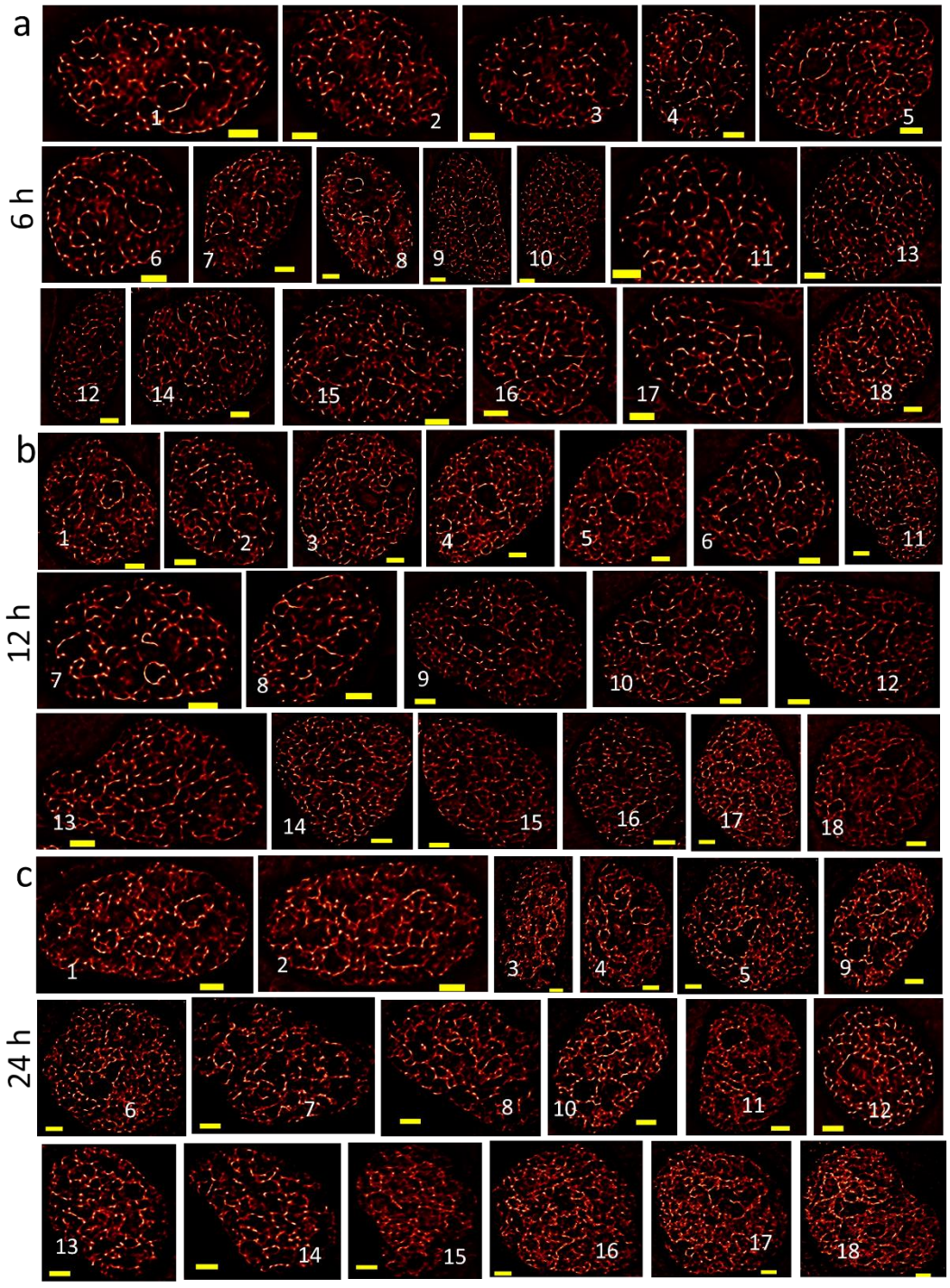

Figure S13: The SRRF images of free DOX (2 µg/mL) treated HeLa cells (n=18 from two independent replicates) at the end of (a) 6 h, (b) 12 h and (c) 24 h using 100x objective (scale bar 3 µm).

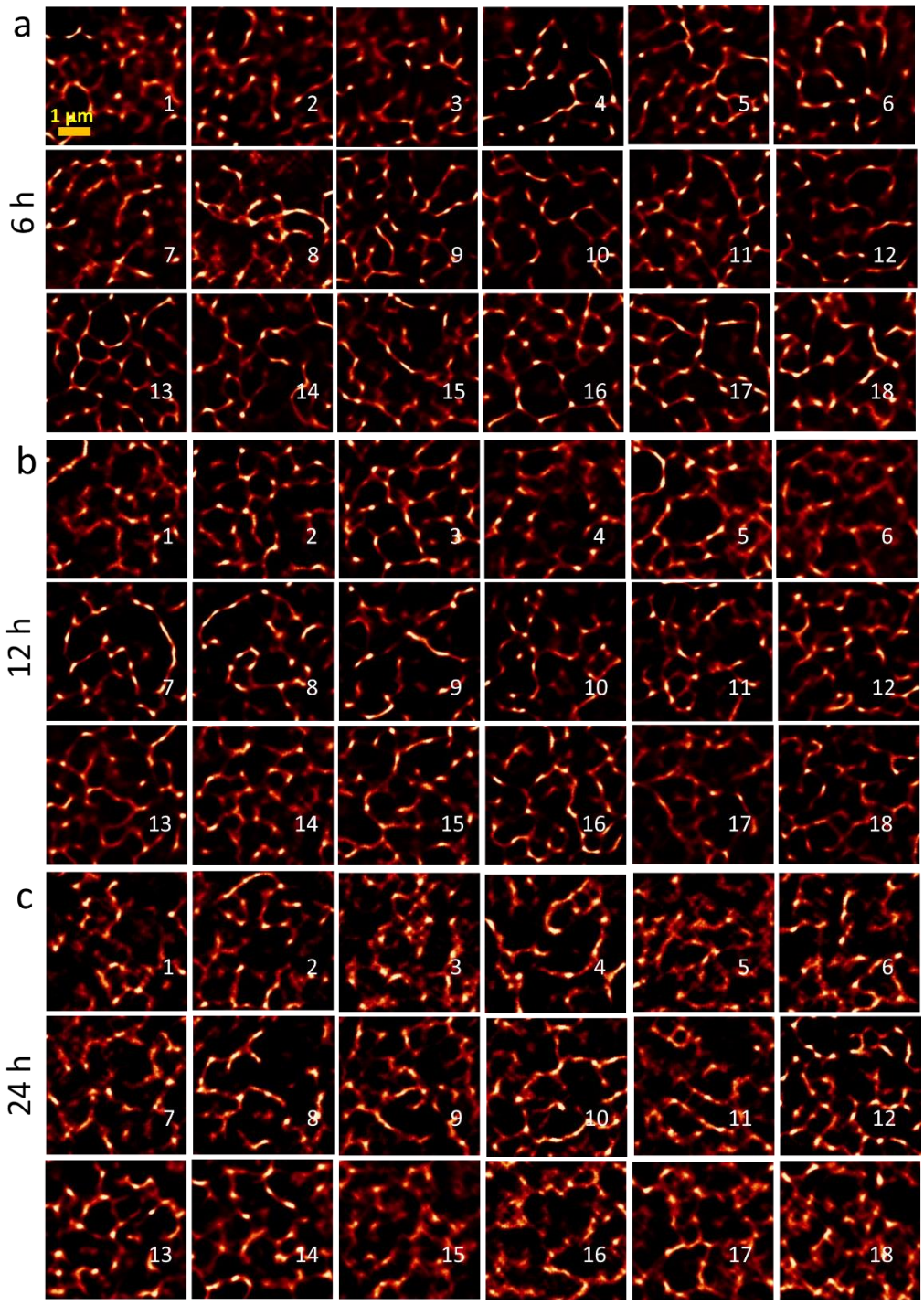

Figure S14: The selected single ROIs from the corresponding full cell SRRF images from Figure S13, of free DOX treated HeLa cells (n=18 from two independent replicates) at the end of (a) 6 h, (b) 12 h and (c) 24 h using 100x objective (scale bar 1 µm, same for all ROIs).

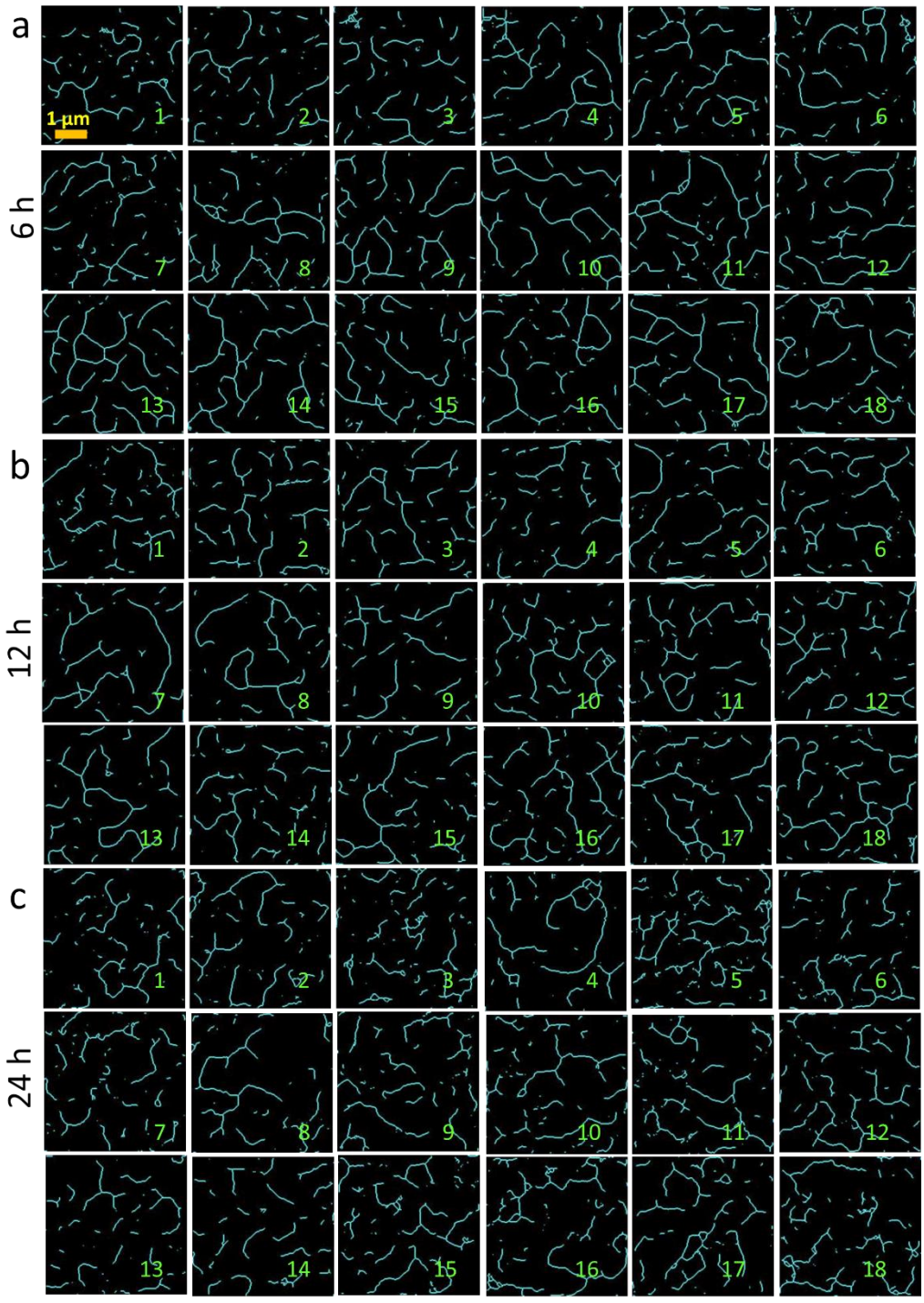

Figure S15: The skeletonized versions of selected single ROIs presented in Figure S14, of free DOX treated HeLa cells (n=18 from two independent replicates) at the end of (a) 6 h, (b) 12 h and (c) 24 h using 100x objective (scale bar 1 µm, same for all ROIs).

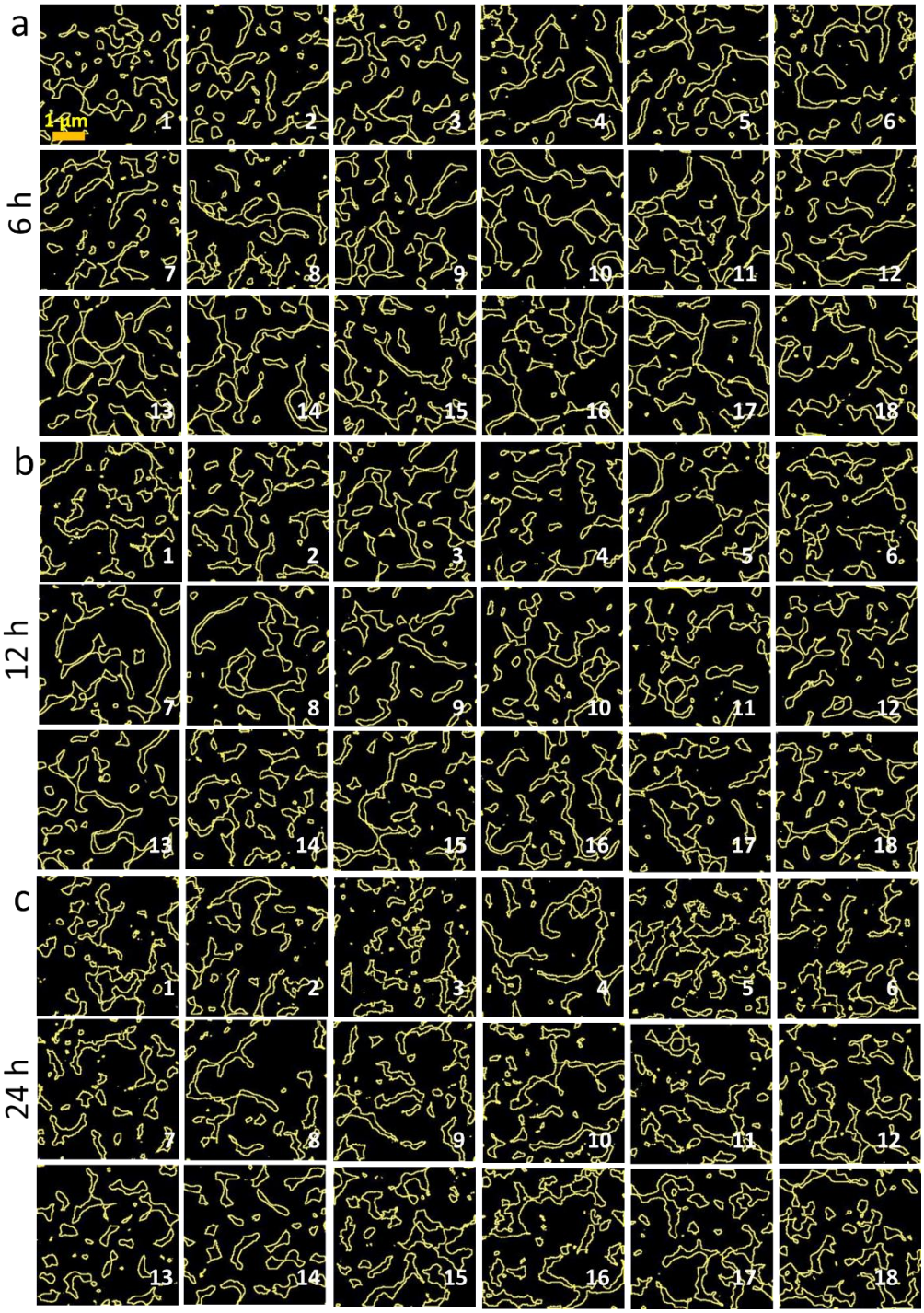

Figure S16: The thresholded, area outlined versions of selected single ROIs presented in Figure S14, of free DOX treated HeLa cells (n=18 from two independent replicates) at the end of (a) 6 h, (b) 12 h and (c) 24 h using 100x objective (scale bar 1 µm, same for all ROIs).

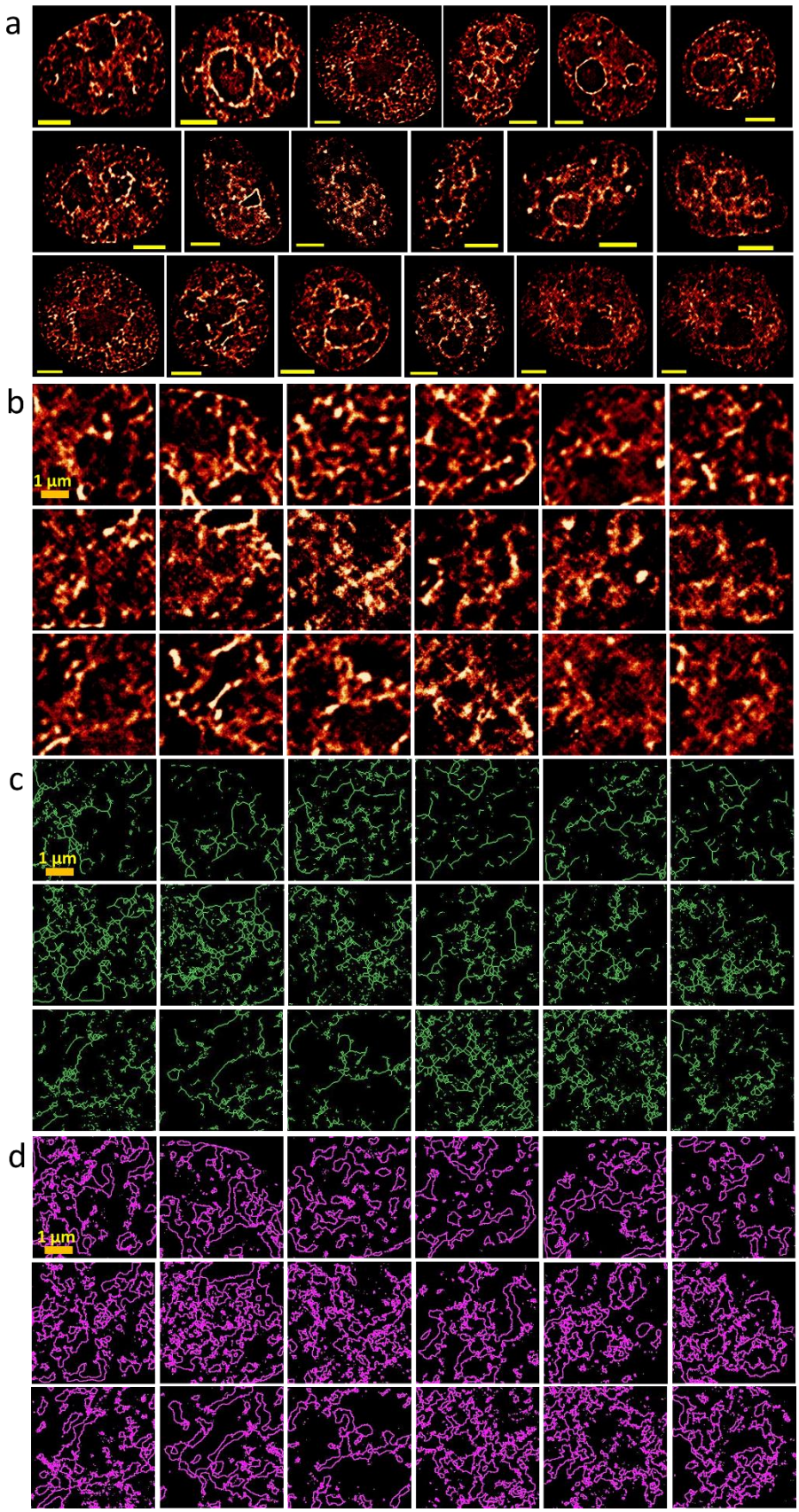

Figure S17: (a) The SRRF images of untreated HeLa cells (n=16 from two independent replicates), stained with DAPI (scale bar 3 µm). (b)The selected single ROIs from the corresponding full cell SRRF

images of (a). (c) The skeletonized versions of selected single ROIs presented in (b). (d) The thresholded, area outlined versions of selected single ROIs presented in (b).